Closed-form expressions for the macroscopic in-plane elastic and creep coefficients of brick masonry

Alberto Taliercio *

Department of Civil and Environmental Engineering, Piazza Leonardo da Vinci 32, 20133 Milan, Italy

Article history:
Received 28 January 2014
Received in revised form 26 March 2014
Available online 2 May 2014

1. Introduction

Predicting the global (or macroscopic, or effective) mechanical properties of heterogeneous media from those of the individual components is a goal that many authors have tried to achieve. The advantages of this approach are manifold. When dealing with fiber reinforced composites, for instance, a material with prescribed macroscopic properties can be designed by properly selecting nature, size and orientation of the fibers. In the case of masonry, tests on full scale specimens are costly and require cumbersome devices. Also, in the case of historic buildings, large specimens are usually impossible to take. Thus, performing tests on brick and mortar samples can be a simpler and feasible alternative, provided that reliable formulas to predict the macroscopic properties of masonry are available.

In linear elasticity, several authors have derived expressions for the effective properties of masonry, which is macroscopically orthotropic if made up by regularly spaced units. This was done e.g., by Pande et al. (1989), who exploited results previously obtained by Salamon (1968) for stratified rock to obtain the five macroscopic elastic constants of masonry, assumed to be represented by an equivalent transversely isotropic material. Later, Pietruszczak and Niu (1992) used an approach typical of the mechanics of composite materials, in which head joints are considered as uniformly dispersed weak inclusions and bed joints as continuous planes of weakness. Refined finite element models, such as those proposed by Anthoine (1995) for periodic masonry, or by Cluni and Gusella (2004) for quasi-periodic masonry, are supposed to predict the macroscopic behavior more accurately. As pointed out by Zucchini and Lourenço (2002), the analytical approaches proposed by Pande et al. (1989) or Pietruszczak and Niu (1992) give unreliable predictions if units and mortar have elastic moduli differing by an order of magnitude or more. Accordingly, these authors proposed approximated displacement (and stress) fields for any Representative Volume Element (RVE), defined by a reduced number of variables, and derived the macroscopic elastic stress–strain law by prescribing approximate equilibrium and compatibility conditions at the boundaries of the different parts of the RVE. Their predictions were found to be sufficiently accurate for any ratio of the elastic moduli of brick and mortar by comparisons with FE analyses. This approach allows closed-form expressions for the macroscopic in- and out-of-plane shear moduli to be obtained, whereas Young's moduli and Poisson's ratios are numerically computed.

The macroscopic behavior of masonry beyond the elastic field was mathematically described by Pietruszczak and Niu (1992), taking into account the elastoplastic behavior of the constituents. Their approach allows the macroscopic failure surface to be determined. Alternatively, an approach based on limit analysis

* Tel.: +39 0223994241; fax: +39 0223994300.
E-mail address: alberto.taliercio@polimi.it

for periodic brickwork can be used to derive these surfaces without any incremental analysis (Milani et al., 2006). Damage effects in the constituents were taken into account e.g., by Luciano and Sacco (1998), Zucchini and Lourenço (2007), and Shieh-Beygi and Pietruszczak (2008), to describe the brittle post-peak behavior experimentally observed in tests on masonry specimens. More recently, Sacco (2009) derived the macroscopic behavior of 2D brickwork in the nonlinear range by assuming damage and friction effects to develop only in the mortar joints, and applying classical homogenization techniques for periodic media to any RVE.

So far, little attention has been devoted to the mathematical description of the long-term behavior of masonry under sustained loads. Indeed, creep effects in masonry are quite significant, as shown by the laboratory tests carried out by Shrive et al. (1997) or by Sayed-Ahmed et al. (1998), and by the evolution of displacements in full-scale buildings monitored by Hughes and Harvey (1995). According to numerical analyses carried out on 3D finite element models of header bond and Flemish bond masonry walls subjected to sustained vertical load (Taliercio, 2013), the time evolution of the vertical macroscopic creep strain turns out to be nearly unaffected by the brick pattern. A simplified 2D layered model is capable to predict the experimentally measured creep strain (Brooks, 1990) with sufficient accuracy for practical purposes. Under stress conditions other than vertical and uniaxial, a layered model might not give reliable predictions.

Despite the importance of creep phenomena, few authors have tried to formulate mathematical expressions for the macroscopic creep coefficients of brick masonry. Brooks (1986), for instance, extended formulas previously proposed in linear elasticity to mathematically define the creep compliance of masonry under sustained vertical stress, by simply replacing the elastic moduli of the constituents by some effective moduli. Recently, Cecchi and Tralli (2012) proposed an analytical model based on homogenization procedures for periodic media; confining creep phenomena into joints and reducing joints to interfaces, closed-form expressions for the macroscopic creep coefficients can be obtained. The reliability of these expressions has still to be assessed, e.g., by comparisons with accurate finite element analyses.

This paper aims at deriving analytical expressions for the macroscopic elastic and creep coefficients of in-plane loaded masonry with regular brick pattern. The proposed approach has similarities with both the so-called Method of Cells (MoC), originally proposed by Aboudi (1991) to predict the macroscopic mechanical behavior of periodic unidirectional fiber-reinforced composites (in the linear elastic, linear viscoelastic and plastic range), and with the already quoted approach employed by Zucchini and Lourenço (2002).

Whereas in other papers dealing with the same subject closed-form expressions only for some of the macroscopic elastic constants are proposed (see Section 3), here all the in-plane elastic constants (Young's moduli, Poisson's ratio and shear modulus) are given analytical expressions. Another novelty of the proposed approach is that also the macroscopic in-plane creep coefficients can be analytically evaluated.

The layout of the paper is as follows. First, in Section 2.1 the fundamentals of homogenization theory for periodic media are briefly recalled. In particular, in Section 2.2 the Reuss and Voigt bounds for the macroscopic elastic stiffness of any heterogeneous medium are specialized to periodic masonry: these bounds will be used in the following sections to define the possible range of variation of any theoretical estimate for the macroscopic elastic constants. Then, in Section 3 a state-of-the-art is presented on some of the closed-form expressions proposed so far for the macroscopic elastic and creep coefficients of masonry. In Section 4 the original approach proposed to derive the macroscopic properties of masonry is illustrated, and applied to estimate the macroscopic in-plane Young's moduli and Poisson's ratio in Section 4.1 and the in-plane shear modulus in Section 4.2. It is shown how the expressions obtained in the elastic field can be extended to describe the macroscopic creep behavior of masonry. In Section 5 the accuracy of the analytical expressions derived in Section 4 is assessed through comparisons with the results of refined finite element analyses and with closed-form expressions available in the literature, recalled in Section 3. Finally, in Section 6 the main findings of the work are summarized and possible future developments are outlined.

A detailed list of the symbols used in the text is provided in Appendix B.

2. Homogenization theory for periodic media: a brief outline

In this section, some fundamental concepts of homogenization theory for periodic media are briefly recalled. Readers are referred e.g., to Nemat-Nasser and Hori (1993) for a detailed discussion on this subject.

2.1. Macroscopic elastic tensor

When dealing with heterogeneous media, it is customary to replace the real medium by a 'homogenized' one and define its global (or macroscopic) properties through the analysis of a Representative Volume Element (RVE). The RVE is the smallest part of the real medium that contains all the information required to completely characterize its average mechanical behavior. If the medium is periodic (as in the case of brickwork with a regular pattern), a single 'unit cell' (V) can be used as RVE. Fig. 1(a) shows a possible choice for the RVE of running bond or header bond brickwork. The macroscopic constitutive law establishes a relationship between macroscopic stresses ($\underline{\underline{\Sigma}}$) and strains ($\underline{\underline{E}}$), which are defined as the volume averages, over the RVE, of the corresponding microscopic variables:

$$\underline{\underline{\Sigma}} = \frac{1}{|V|}\int_V \underline{\underline{\sigma}}(\underline{x})dV, \quad \underline{\underline{E}} = \frac{1}{|V|}\int_V \underline{\underline{\epsilon}}(\underline{x})dV. \tag{1}$$

In particular, as the microscopic strain $\underline{\underline{\epsilon}}$ must be periodic, neglecting rigid body motions the microscopic displacement field $\underline{u}$ must be of the form

$$\underline{u} = \underline{\underline{E}} \cdot \underline{x} + \tilde{\underline{u}}, \tag{2}$$

where $\tilde{\underline{u}}$ is periodic over V. Fig. 1(b) and (c) shows RVE's deformed according to Eq. (2) under macroscopic vertical compression and shear, respectively.

In linear elasticity, the macroscopic constitutive law can be alternatively written as $\underline{\underline{\Sigma}} = \underline{\underline{\underline{\underline{D}}}}^{hom} : \underline{\underline{E}}$, or as $\underline{\underline{E}} = \underline{\underline{\underline{\underline{C}}}}^{hom} : \underline{\underline{\Sigma}}$. $\underline{\underline{\underline{\underline{D}}}}^{hom}$ denotes the macroscopic stiffness tensor, and $\underline{\underline{\underline{\underline{C}}}}^{hom}$ its inverse (also called macroscopic flexibility tensor). In the 2D case, assuming masonry to be macroscopically orthotropic, both tensors are defined by four independent elastic constants. From here onwards, x_1 denotes an axis parallel to the bed joints and to the mid-plane of the wall, x_2 an axis parallel to the head joints and to the mid-plane of the wall, and x_3 an axis parallel to the wall thickness (see Fig. 1(a)). Under in-plane stress, and assuming plane stress conditions, the macroscopic elastic constitutive law can be written as

$$\begin{pmatrix} E_{11} \\ E_{22} \\ 2E_{12} \end{pmatrix} = \begin{pmatrix} 1/E_1 & -\nu_{21}/E_2 & 0 \\ -\nu_{12}/E_1 & 1/E_2 & 0 \\ 0 & 0 & 1/G_{12} \end{pmatrix} \begin{pmatrix} \Sigma_{11} \\ \Sigma_{22} \\ \Sigma_{12} \end{pmatrix}, \tag{3}$$

where E_1 and E_2 are macroscopic Young's moduli, ν_{12} and ν_{21} are macroscopic Poisson's ratios (with $\nu_{12}/E_1 = \nu_{21}/E_2$), and G_{12} is the macroscopic in-plane shear modulus.

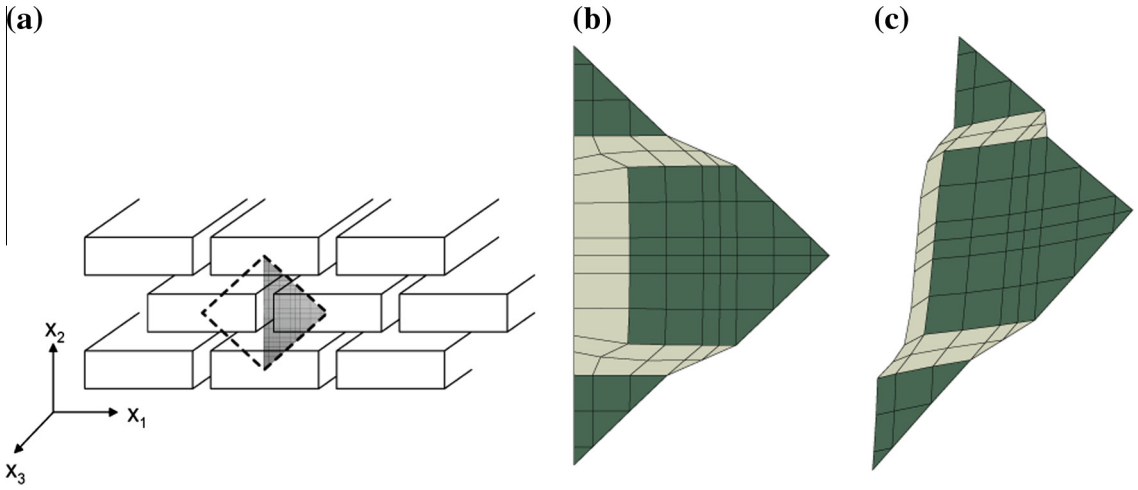

Fig. 1. (a) RVE of any periodic running bond or header bond-type brickwork. (b) Deformed RVE under macroscopic in-plane vertical compression. (c) Deformed RVE under macroscopic in-plane shear.

In principle, $\underline{\underline{\underline{\underline{D}}}}^{hom}$ (or $\underline{\underline{\underline{\underline{C}}}}^{hom}$) can be obtained computing the total potential energy of the RVE, Π^{hom}, under any macroscopic stress:

$$\Pi^{hom} = \min_{\underline{u}\in Y_{per}} \Pi = \min_{\underline{u}\in Y_{per}} \left(\frac{1}{2|V|} \int_V \underline{\underline{\epsilon}}(\underline{u}) : \underline{\underline{\underline{\underline{d}}}} : \underline{\underline{\epsilon}}(\underline{u}) dV - \underline{\underline{\Sigma}} : \int_V \underline{\underline{\epsilon}}(\underline{u}) dV \right), \tag{4}$$

where Y_{per} is the set of the strain-periodic microscopic displacement fields and $\underline{\underline{\underline{\underline{d}}}}$ is the microscopic elasticity tensor, assumed to be piecewise constant in the two phases of the RVE. $\underline{\underline{\underline{\underline{c}}}} = \underline{\underline{\underline{\underline{d}}}}^{-1}$ will denote the elastic flexibility tensor. As

$$\Pi^{hom} = \frac{1}{2}\underline{\underline{E}} : \underline{\underline{\underline{\underline{D}}}}^{hom} : \underline{\underline{E}} - \underline{\underline{\Sigma}} : \underline{\underline{E}} = -\frac{1}{2}\underline{\underline{E}} : \underline{\underline{\underline{\underline{D}}}}^{hom} : \underline{\underline{E}} = -\frac{1}{2}\underline{\underline{\Sigma}} : \underline{\underline{\underline{\underline{C}}}}^{hom} : \underline{\underline{\Sigma}} \tag{5}$$

for a given macroscopic stress $\underline{\underline{\Sigma}}$ any strain-periodic displacement field gives an upper bound for the macroscopic elastic 'stiffness' $\underline{\underline{\underline{\underline{D}}}}^{hom}$ (and, conversely, a lower bound for the macroscopic elastic 'flexibility' $\underline{\underline{\underline{\underline{C}}}}^{hom} = (\underline{\underline{\underline{\underline{D}}}}^{hom})^{-1}$).

2.2. Reuss and Voigt bounds

Let η_m and η_b denote the volume fractions of mortar and bricks in any RVE, respectively. Assuming in-plane stresses to be uniform over the RVE, a lower bound (or Reuss-type approximation) for the macroscopic Young's moduli E_1 and E_2 is obtained:

$$E^{Reuss} = \frac{E_m}{\eta_m + \eta_b \alpha_E}, \tag{6}$$

with $\alpha_E = E_m/E_b$, whereas a lower bound for the macroscopic shear modulus G_{12} is

$$G_{12}^{Reuss} = \frac{G_m}{\eta_m + \eta_b \alpha_G} \tag{7}$$

with $\alpha_G = G_m/G_b$. Using a Reuss-type uniform stress field, one also gets an approximated value for the macroscopic in-plane Poisson's ratio:

$$\nu_{12}^{Reuss} = \frac{\eta_m \nu_m + \eta_b \alpha_E \nu_b}{\eta_m + \eta_b \alpha_E}. \tag{8}$$

Conversely, assuming in-plane strains to be uniform over the RVE, an upper bound (or Voigt-type approximation) for the macroscopic Young's moduli E_1 and E_2 is obtained:

$$E^{Voigt} = \frac{\left(\eta_m \frac{E_m}{1-\nu_m} + \eta_b \frac{E_b}{1-\nu_b}\right)\left(\eta_m \frac{E_m}{1+\nu_m} + \eta_b \frac{E_b}{1+\nu_b}\right)}{\eta_m \frac{E_m}{1-\nu_m^2} + \eta_b \frac{E_b}{1-\nu_b^2}}, \tag{9}$$

whereas an upper bound for the macroscopic shear modulus G_{12} is

$$G_{12}^{Voigt} = \eta_m G_m + \eta_b G_b = G_m \left(\eta_m + \frac{\eta_b}{\alpha_G} \right). \tag{10}$$

Finally, the Voigt-type approximation for the macroscopic in-plane Poisson's ratio reads

$$\nu_{12}^{Voigt} = \frac{\eta_m \alpha_E \nu_m (1-\nu_b^2) + \eta_b \nu_b (1-\nu_m^2)}{\eta_m \alpha_E (1-\nu_b^2) + \eta_b (1-\nu_m^2)}. \tag{11}$$

When applied to the prediction of the global creep behavior of two-phase materials, according to the Reuss approximation the macroscopic creep strain is simply the volume average of the creep strains of the two phases, which are constant over each phase. Assuming the Poisson's ratios of each phase to be constant in time (Brooks, 1990), only the creep function under uniaxial stress ($J_m(t), J_b(t)$) has to be known to define the time evolution of all the strain components under any sustained stress. A Reuss-type approximation for the homogenized creep function is

$$J^{Reuss}(t) = \eta_m J_m(t) + \eta_b J_b(t). \tag{12}$$

Conversely, a rule-of-mixture-type approximation for the homogenized relaxation function can be obtained using the Voigt model:

$$R^{Voigt}(t) = \eta_m R_m(t) + \eta_b R_b(t). \tag{13}$$

The creep function of the homogenized material according to the Voigt model can be obtained from Eq. (13), knowing that the creep function is the inverse of the relaxation function in the sense of Carson transforms (Park and Schapery, 1999). In general, the analytical expression (if any) of the Voigt-type approximated creep function is quite awkward and of little use in practice. This is because the stress in the two phases varies in time, although the macroscopic stress is constant, and the strain in each phase is given by a convolution integral (see e.g., Park and Schapery, 1999). Accordingly, some authors circumvent this difficulty and adopt an 'effective modulus' to describe the time evolution of the strain in each phase (Bažant, 1972). This method is also used by many codes of practice. With this approximation, the Voigt-type approximated creep function can be obtained by Eq. (9) and reads

$$J^{Voigt}(t) = J_m(t)\frac{\frac{\eta_m}{1-\nu_m^2}+\frac{\eta_b}{(1-\nu_b^2)\alpha_E(t)}}{\left(\frac{\eta_m}{1-\nu_m}+\frac{\eta_b}{(1-\nu_b)\alpha_E(t)}\right)\left(\frac{\eta_m}{1+\nu_m}+\frac{\eta_b}{(1+\nu_b)\alpha_E(t)}\right)} \tag{14}$$

with $\alpha_E(t) = J_b(t)/J_m(t)$. The difference between the real evolution of the stress in time and the predictions given by the effective elastic modulus method is discussed e.g., by Reda Taha and Shrive (2006).

3. State-of-the art

The simplest model to estimate the macroscopic elastic properties of brick masonry according to those of its constituents is a layered model, where head joints are neglected and homogeneous brick layers are alternated with horizontal mortar joints. This elementary model is occasionally quoted for comparison purposes (see e.g., Anthoine, 1995), and was find to give satisfactory results as far as the short- and the long-term behavior of vertically loaded walls is concerned (Taliercio, 2013). Assuming stresses and strains to be uniform over each layer, the macroscopic in-plane elastic constants of masonry can be easily computed by hand through equilibrium and compatibility conditions, and read

$$E_1^{lay} = E_m(p_1+p_2/\alpha_E),\ E_2^{lay} = E_1^{lay}\left(p_1^2+p_2^2+p_1p_2\left(2\nu_m\nu_b+(1-\nu_b^2)\alpha_E + (1-\nu_m^2)/\alpha_E\right)\right)^{-1}, \nu_{12}^{lay} = p_1\nu_m+p_2\nu_b,\ G_{12}^{lay} = G_m(p_1+p_2\alpha_G)^{-1}, \tag{15}$$

where $p_1 = \alpha_h/(1+\alpha_h)$ and $p_2 = 1/(1+\alpha_h)$.

An alternative approach was followed by Salamon (1968) for stratified rock masses formed by transversely isotropic layers, defining stresses and strains in each layer as the sum of the macroscopic variable and an auxiliary component. When applied to isotropic brick and mortar layers, Salamon's model gives

$$E_1^{Salamon} = (1-\bar{\nu}^2)\sum_{i=1}^{2}\frac{p_iE_i}{1-\nu_i^2},\ E_2^{Salamon} = \left(\sum_{i=1}^{2}\frac{p_i}{E_i}\left(1-\frac{2\nu_i^2}{1-\nu_i}\right)+\frac{2(\nu_{12}^{Salamon})^2}{(1-\bar{\nu})E_1^{Salamon}}\right)^{-1},$$
$$\nu_{12}^{Salamon} = (1-\bar{\nu})\sum_{i=1}^{2}\frac{p_i\nu_i}{1-\nu_i},\ G_{12}^{Salamon} = G_{12}^{lay}, \tag{16}$$

where subscript $i = 1$ refers to mortar, $i = 2$ refers to brick and

$$\bar{\nu} = \frac{\sum_{i=1}^{2}\frac{p_i\nu_iE_i}{1-\nu_i^2}}{\sum_{i=1}^{2}\frac{p_iE_i}{1-\nu_i^2}}. \tag{17}$$

More refined models take the presence of head joints into account, with different degrees of accuracy. A composite model for elasticity, creep and shrinkage of masonry was developed by Brooks (1986, 1990), representing masonry as an assemblage of a brick/vertical (head) mortar joint and a horizontal (bed) mortar joint. Strain is assumed to be constant over each element; bonding between brick and mortar joints is neglected, and so are Poisson's effects. Accordingly, the 'modulus of elasticity' of any masonry wall under vertical stresses can be estimated, and is found to depend on the number of courses (C) and the number of bricks along the wall width (B):

$$\frac{1}{E_2^{Brooks}} = \frac{Ch_b}{H}\frac{W}{b_bBE_{by}+b_m(B-1)E_m}+\frac{h_m(C+1)}{HE_m}, \tag{18}$$

being H and W the total wall height and width, respectively, and E_{by} the vertical Young's modulus of bricks. In particular, if both C and B are large (which is consistent with the concept of RVE) and neglecting brick anisotropy, the vertical modulus of elasticity is approximately given by

$$E_2^{Brooks} = E_m\frac{(1+\alpha_h)(1+\alpha_E\alpha_b)}{\alpha_E(1+\alpha_b(1+\alpha_h))+\alpha_h} \tag{19}$$

(refer to Appendix B for the meaning of the symbols). Considering Young's moduli as effective moduli, Brooks employed Eq. (19) to predict also masonry creep strains.

Pande et al. (1989) proposed a sort of two-step homogenization model, where the equivalent properties of a layer consisting of units and head joints are first derived using Eqs. (16); second, the equivalent properties of a layered medium consisting of bed joints and the previously homogenized brick–mortar system are obtained using the same expressions. Here again, closed-form expressions for the macroscopic constants of the homogenized orthotropic medium can be obtained. The expressions of the four constants obtained by Pande et al. (1989) for plane stress are reported in Appendix A. Readers are referred to the original paper for further details.

A similar approach was followed by Pietruszczak and Niu (1992), who also perform a two-step homogenization. The first step refers to brick courses, in which head joints are considered as aligned, evenly spaced inclusions uniformly dispersed in a matrix. The average properties of the courses are derived by Mori–Tanaka's mean-field theory, based on the concept of Eshelby's tensor (see e.g., Nemat-Nasser and Hori (1993)): the results obtained by Zhao and Weng (1990) for composites reinforced by aligned elliptical cylinders are employed in this step. In the second step, macroscopic stresses and strains in the homogenized medium equivalent to the layered one are defined by a rule of mixtures. The approach covers both the linear elastic and the elasto-plastic range.

More recently, Zucchini and Lourenço (2002) subdivided a typical representative unit cell of masonry into sub-cells, corresponding to bricks, bed joints, head joints and the intersections of these joints (also referred to as 'cross joints'). The expressions proposed for the stress and strain fields within each of the sub-cells fulfill the equilibrium and compatibility conditions almost everywhere. They provided closed-form expressions for the three macroscopic shear moduli of masonry: in particular, the macroscopic in-plane shear modulus can be cast in the form

$$G_{12}^{ZL} = G_m\left(1+\frac{(1-\alpha_G)(1-\alpha_b\alpha_h)(1+\nu_m+2\alpha_B)}{(\alpha_h+\alpha_G)((1+\alpha_b)(1+\nu_m)+2\alpha_B)+2\alpha_b\alpha_B(1+\alpha_h(2-\alpha_G))}\right). \tag{20}$$

No explicit analytical expression is provided for the macroscopic Young's moduli and Poisson's ratios, as the authors claim that they are of a form too complex to be used for practical purposes.

4. A Method-of-Cells-type approach for the determination of the macroscopic and creep coefficients of masonry

The Method of Cells (MoC) was originally proposed by Aboudi (1991) for unidirectional composites, reinforced by a regular pattern of long, reinforcing fibers. The method allows the macroscopic elastic and creep coefficients and the macroscopic strength properties of fiber reinforced composites (FRCs) to be computed in closed form, according to the elastic and strength properties of fibers, matrix and interface.

The method comprises the following points:

1. fibers have square cross-section, and are arranged in a doubly periodic array in any plane perpendicular to their axis;
2. any RVE is subdivided into four sub-cells, and the displacement within each sub-cell is supposed to be a linear function of the in-plane coordinates;
3. displacements averaged over any interface between adjacent sub-cells are continuous;
4. interface tractions computed according to the average stresses in each sub-cell are continuous;

5. the composite constitutive equations are obtained expressing the stresses averaged over the RVE (i.e. the macroscopic stresses) in terms of averaged (or macroscopic) strains.

Here, a somehow similar approach is proposed for brick masonry, with the aim of obtaining the macroscopic elastic and creep coefficients in closed form. The analysis is limited to the 2D case, which means that only the behavior under in-plane loads is considered. Whereas in the original MoC any RVE is assumed to be in a generalized plane strain state, for in-plane loaded masonry plane stress conditions are considered: a discussion on the admissibility of this assumption for different types of brickwork can be found in Anthoine (1997).

Note first of all that point No. 1 must be generalized because of the rectangular shape of the brick section. Point No. 2 could be acceptable only for stack-bond masonry, but must be modified to take into account more common types of masonry with staggered brick patterns. In the present work, header bond and running (or stretcher) bond brickworks will be dealt with (see Fig. 1(a)). Unlike the rhomboidal RVE used for FE analyses (see Fig. 1(b) and (c)), here it is expedient to use a RVE of rectangular shape, which is subdivided into six sub-cells as shown in Fig. 2. Sub-cell No. 1 consists of brick; sub-cell No. 2 is a head joint; sub-cells 3 and 4 pertain to a bed joint; sub-cells 5 and 6 are intersections of bed and head joints (or 'cross joints'). More complex brick patterns (e.g., Flemish bond or English bond) require a different choice for the RVE, because of the coexistence of stretchers and headers in the wall.

Similarly to the MoC, a strain-periodic piecewise differentiable displacement field is proposed over the RVE, which depends on a limited number of parameters (or 'degrees of freedom', d.o.f.s). The displacements within each sub-cell are linear (albeit not affine) functions of the in-plane coordinates. Continuity of the interface displacements is automatically fulfilled (see point No. 3).

It is worth noting that a similar approach was followed by Luciano and Sacco (1998), who formulated a microscopic displacement field defined by eight d.o.f.s in each sub-cell. Out-of-plane displacements and damage effects in both components were also taken into account. No analytical expression for the macroscopic elastic and creep coefficients was provided by these authors, owing to the complex kinematics of the RVE.

Two different approaches are proposed here to derive the macroscopic constitutive law of masonry. In the first one, which is basically consistent with the original MoC, continuity of the interface tractions is fulfilled almost everywhere, except for the boundaries of the cross joints, provided that the d.o.f.s fulfill suitable relationships (point No. 4). The equilibrium conditions within the sub-cells are also fulfilled everywhere, except for the cross joints. As the cross joints are usually small, the approximations made are expected to be acceptable. Finally (point No. 5), stresses and strains

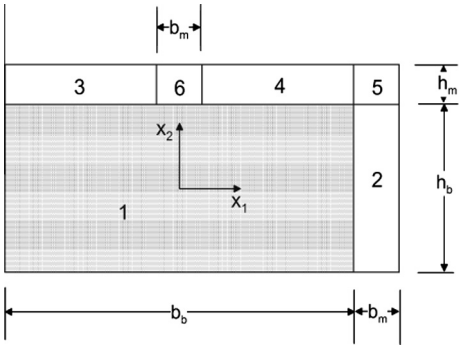

Fig. 2. Subdivision of any RVE into sub-cells.

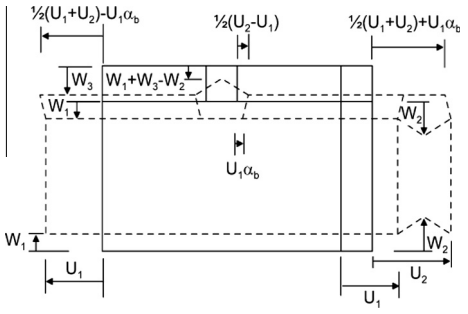

Fig. 3. Strain-periodic kinematically admissible microscopic strain field under horizontal or vertical macroscopic stresses.

computed according to the remaining d.o.f.s are averaged over the RVE and the macroscopic constitutive law is obtained. In the second approach, the values of the d.o.f.s are derived by minimizing the macroscopic potential energy of the RVE, Eq. (4), considered as a 'structure' subjected to any given 'load', corresponding to the macroscopic stress $\underline{\underline{\Sigma}}$. The macroscopic strain tensor $\underline{\underline{E}}$ corresponding to $\underline{\underline{\Sigma}}$ is obtained, and an approximation for the macroscopic elasticity tensor $\underline{\underline{\underline{\underline{D}}}}^{hom}$ is computed. Accordingly, upper bounds for the real macroscopic elastic and shear moduli are obtained in linear elasticity. From the elastic coefficients obtained with the two approaches, approximated creep coefficients are also obtained using the concept of 'effective moduli' (see Section 2).

4.1. Instantaneous and delayed behavior under normal stresses

Consider the deformed RVE shown in Fig. 1(b), corresponding to the FE solution obtained under in-plane macroscopic normal stresses parallel either to the bed or to the head joints, Σ_{11} or Σ_{22}. Let the origin of the reference frame (Ox_1x_2) be placed at the center of sub-cell No. 1 (brick). A piecewise differentiable strain-periodic

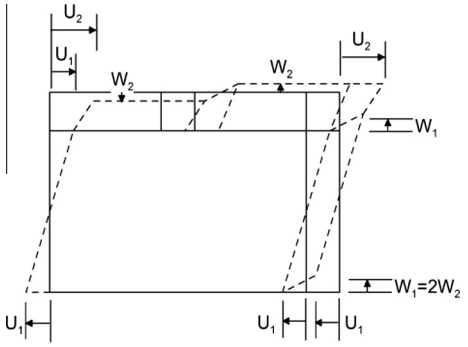

Fig. 4. Strain-periodic kinematically admissible microscopic strain field under in-plane macroscopic shear.

Table 1
Values of the geometrical and mechanical parameters employed in Figs. 5 and 6 and in Table 2.

Fig.	h_m (mm)	h_b (mm)	b_m (mm)	b_b (mm)	E_b (MPa)	G_b (MPa)
5	10	55	10	120	Variable	Variable
6	Variable	55	$= h_m$	120	17100	7434.8

displacement field, which approximates the FE solution reasonably well, can be formulated as follows:

$$u_1^{(1)} = 2U_1\frac{x_1}{b_b},\quad u_2^{(1)} = -2W_1\frac{x_2}{h_b};$$

$$u_1^{(2)} = U_1 + \frac{(U_2-U_1)(x_1-b_b/2)}{b_m},\quad u_2^{(2)} = -2\frac{x_2}{h_b}\left(\frac{2(W_1-W_2)\left|\frac{b_m+b_b}{2}-x_1\right|}{b_m}+W_2\right);$$

$$u_1^{(3)} = u_1^{(1)} - \frac{(U_1(1+2\alpha_b)-U_2)(\frac{h_b}{2}-x_2)}{2h_m},\quad u_2^{(3)} = -W_1 + \frac{(W_1-W_3)(x_2-h_b/2)}{h_m};$$

$$u_1^{(4)} = u_1^{(1)} + \frac{(U_1(1+2\alpha_b)-U_2)(\frac{h_b}{2}-x_2)}{2h_m},\quad u_2^{(4)} = u_2^{(3)}; \tag{21}$$

$$u_1^{(5)} = U_1 - \frac{(U_1(1+2\alpha_b)-U_2)\left(\frac{b_b+b_m}{2}-x_1\right)\left(x_2-\frac{h_b}{2}\right)}{b_m h_m} - \frac{(U_1-U_2)\left(x_1-\frac{b_b}{2}\right)}{b_m},$$

$$u_2^{(5)} = -W_3\frac{x_2-\frac{h_b}{2}}{h_m} - 2\frac{\left(W_2\frac{b_m}{2}-(W_2-W_1)\left|\frac{b_b+b_m}{2}-x_1\right|\right)\left(\frac{h_b}{2}+h_m-x_2\right)}{b_m h_m};$$

$$u_1^{(6)} = 2\frac{x_1}{b_b}\left(U_1 - \frac{\left(U_1+\frac{U_1-U_2}{2\alpha_b}\right)\left(x_2-\frac{h_b}{2}\right)}{h_m}\right),$$

$$u_2^{(6)} = -W_1 + \frac{\left(W_2-W_3+2(W_1-W_2)\frac{|x_1|}{b_m}\right)\left(x_2-\frac{h_b}{2}\right)}{h_m}. \tag{22}$$

This field is defined by five d.o.f.s $(U_1, U_2, W_1, W_2, W_3)$, shown in Fig. 3. The macroscopic strains associated with the microscopic displacement field (21) are simply

$$E_{11} = \frac{1}{|V|}\int_V \epsilon_{11}dV = \frac{U_1+U_2}{b_b+b_m},\quad E_{22} = \frac{1}{|V|}\int_V \epsilon_{22}dV = -\frac{W_1+W_3}{h_b+h_m}. \tag{23}$$

Note that the 'hidden' d.o.f. W_2 does not affect the macroscopic strains (and the relevant macroscopic stresses). It might be used to enrich the modeling of the local strain and stress field. For present purposes, it can be taken equal to W_1: this choice has the advantage of fulfilling equilibrium conditions parallel to the interface between brick and head joint. Additionally, setting $W_1 = W_2$ stresses and strains are uniform over the sub-cells, except for the cross joints (sub-cells 5 and 6). Within these sub-cells, equilibrium along x_2 for an infinitesimal element is not fulfilled.

Relationships between U_2, W_3 and between U_1, W_1 can be found by prescribing that equilibrium along the normal to the interfaces between brick and both joints is fulfilled:

$$\sigma_{11}^{(1)} = \sigma_{11}^{(2)} \Rightarrow U_2 = U_1\left(1+\frac{2\alpha_b(1-\nu_m^2)}{\alpha_E(1-\nu_b^2)}\right) + 2W_1\frac{\alpha_h}{\alpha_m}\left(\nu_m - \frac{\nu_b(1-\nu_m^2)}{\alpha_E(1-\nu_b^2)}\right),$$

$$\sigma_{22}^{(1)} = \sigma_{22}^{(3)} \Rightarrow W_3 = 2U_1\alpha_b\alpha_m\left(\nu_m - \frac{\nu_b(1-\nu_m^2)}{\alpha_E(1-\nu_b^2)}\right) + W_1\left(1+\frac{2\alpha_h(1-\nu_m^2)}{\alpha_E(1-\nu_b^2)}\right). \tag{24}$$

Equilibrium is not fulfilled at the interface between brick and bed joint parallel to the interface and along the boundary of the cross joints perpendicularly to the interfaces.

The remaining d.o.f.s can be related to the macroscopic in-plane strains through Eqs. (23) and (24):

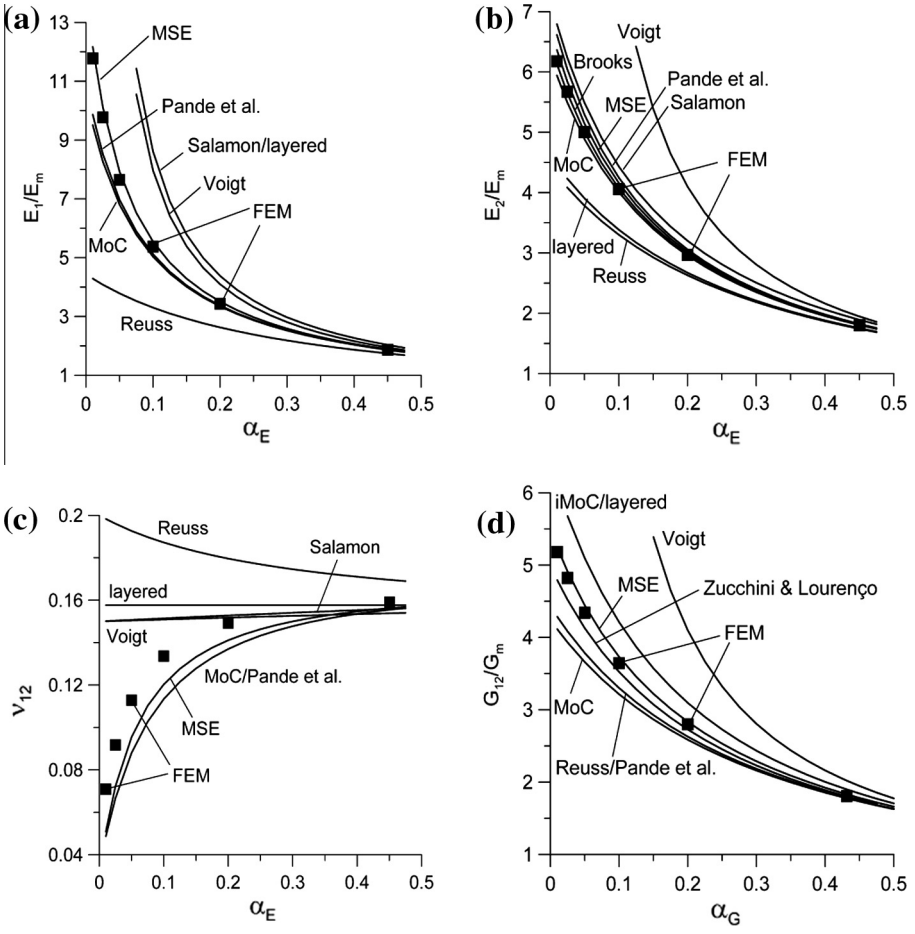

Fig. 5. Header bond brickwork: predicted values of the macroscopic in-plane elastic constants vs. mortar-to-brick stiffness ratio. (a) E_1, (b) E_2, (c) ν_{12}, and (d) G_{12}.

$$U_1 = \frac{h_m \alpha_E \left(E_{11}(1+\alpha_b)(\alpha_h(1-\nu_m^2)+\alpha_E(1-\nu_b^2)) - E_{22}\alpha_b(1+\alpha_h)(\nu_b(1-\nu_m^2)-\alpha_E\nu_m(1-\nu_b^2))\right)}{2\alpha_b\alpha_m\left(\alpha_E(\alpha_E(1-\nu_b^2)+\alpha_h(1-\nu_m^2))+\alpha_b(\alpha_E(1+2\alpha_h\nu_b\nu_m)(1-\nu_m^2)+\alpha_h(1-\nu_m^2)^2-\alpha_E^2\alpha_h(1-\nu_b^2)\nu_m^2)\right)},$$

$$W_1 = \frac{h_m \alpha_E \left(E_{11}(1+\alpha_b)\alpha_h(\nu_b(1-\nu_m^2)-\alpha_E(1-\nu_b^2)\nu_m) - E_{22}(1+\alpha_h)(\alpha_b(1-\nu_m^2)+\alpha_E(1-\nu_b^2))\right)}{2\alpha_h\left(\alpha_E(\alpha_E(1-\nu_b^2)+\alpha_h(1-\nu_m^2))+\alpha_b(\alpha_E(1+2\alpha_h\nu_b\nu_m)(1-\nu_m^2)+\alpha_h(1-\nu_m^2)^2-\alpha_E^2\alpha_h(1-\nu_b^2)\nu_m^2)\right)}. \tag{25}$$

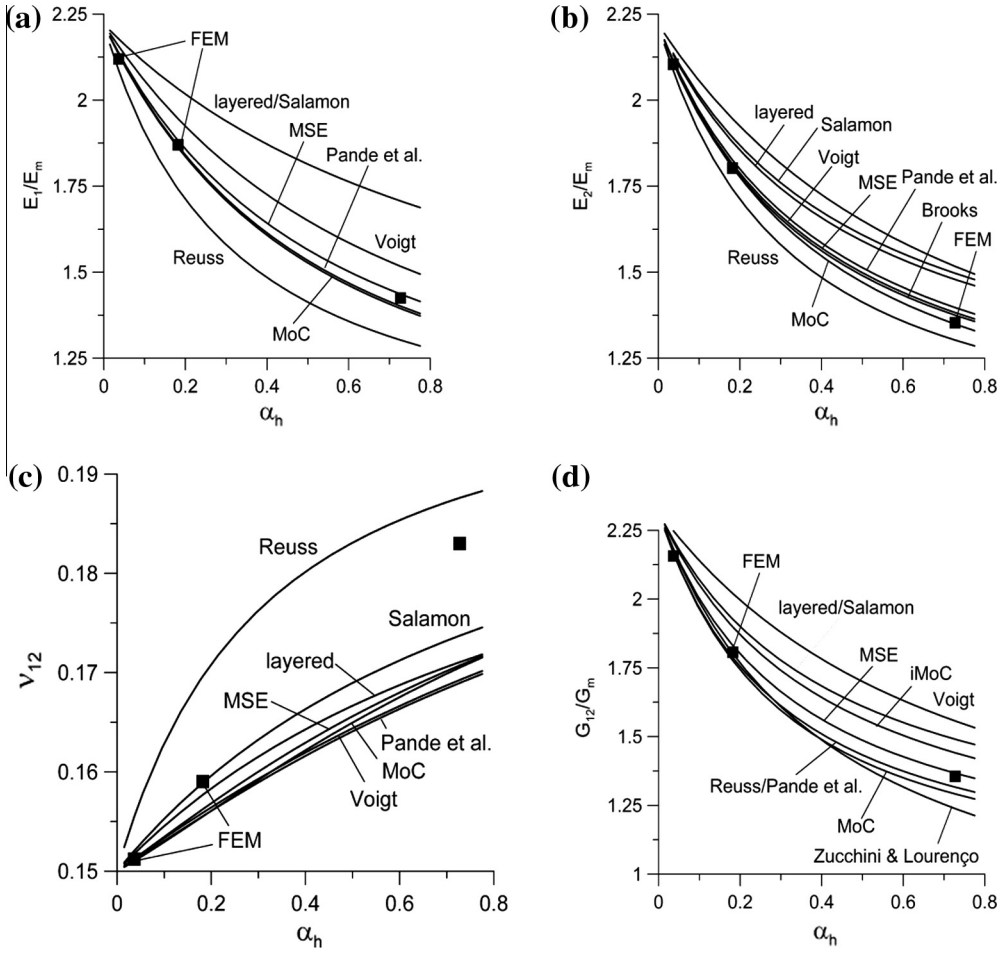

Fig. 6. Header bond brickwork: predicted values of the macroscopic in-plane elastic constants vs. bed joint thickness-to-brick height ratio. (a) E_1, (b) E_2, (c) ν_{12}, and (d) G_{12}.

Finally, computing the macroscopic in-plane stresses Σ_{11} and Σ_{22}, the macroscopic elasticity constants can be identified. Setting $\Sigma_{22} = 0$, one gets

$$E_1^{(MoC)} = \frac{\Sigma_{11}}{E_{11}} = E_m\left(1+\frac{d_1-\alpha_b d_2}{d_3+\alpha_b d_2}\right), \quad \nu_{12}^{(MoC)} = -\frac{E_{22}}{E_{11}} = \frac{(1+\alpha_b)d_5}{(1+\alpha_b)d_4+\alpha_b d_2}, \tag{26}$$

whereas, setting $\Sigma_{11} = 0$, one gets

$$E_2^{(MoC)} = \frac{\Sigma_{22}}{E_{22}} = E_m\left(1+\frac{d_1-\alpha_h d_2}{d_3+\alpha_h d_2}\right), \quad \nu_{21}^{(MoC)} = -\frac{E_{11}}{E_{22}} = \frac{(1+\alpha_h)d_5}{(1+\alpha_h)d_4+\alpha_h d_2}, \tag{27}$$

with

$$\begin{aligned} d_1 &= (1-\alpha_E)(1+\alpha_h)(1+\alpha_b-\nu_m^2) - \alpha_b((1-\alpha_E)(1+\alpha_E\alpha_h) \\ &\quad + (\alpha_E\nu_b-\nu_m)^2\alpha_h)\nu_m^2, \\ d_2 &= \left((1-\alpha_E)^2-(\nu_m-\alpha_E\nu_b)^2\right)(1-\nu_m^2), \\ d_3 &= d_4(1+\alpha_b+\alpha_h)+(d_2+d_4)\alpha_b\alpha_h, \\ d_4 &= \alpha_E(1+\alpha_b+\alpha_h+2\alpha_b\alpha_h\nu_b\nu_m)(1-\nu_m^2) \\ &\quad + \alpha_b\alpha_h\left((1-\nu_m^2)^2-\alpha_E^2(1-\nu_b^2)\nu_m^2\right), \\ d_5 &= \nu_m d_4 + \alpha_E(\nu_b-\nu_m)(1-\nu_m^2). \end{aligned} \tag{28}$$

It can be shown that $\nu_{12}E_2 = \nu_{21}E_1$, conforming with the symmetry of the macroscopic elasticity tensor.

Table 2
Macroscopic elastic constants computed according to different methods for header bond and running bond brickwork. In brackets: percent difference with respect to Abaqus predictions.

		E_1 (MPa)	E_2 (MPa)	ν_{12}	G_{12} (MPa)
Header bond	Abaqus	14401.2	13877.6	0.1590	5796.1
	Reuss	13409.5 (−6.9)	13409.5 (−3.4)	0.1696 (+6.7)	5732.4 (−1.1)
	Voigt	14984.8 (+4.1)	14984.8 (+8.0)	0.1559 (−2.0)	6482.0 (+11.8)
	Salamon	15656.7 (+8.7)	14565.3 (+5.0)	0.1589 (−0.1)	6181.9 (+6.7)
	Brooks	–	13912.7 (+0.3)	–	–
	Pande et al.	14374.8 (−0.2)	14028.5 (+1.1)	0.1555 (−2.2)	5732.4 (−1.1)
	Zucchini & Lourenço	–	–	–	5780.8 (-0.3)
	MoC	14336.6 (−0.4)	13891.0 (+0.1)	0.1555 (−2.2)	6092.1* (+5.1)
	MSE	14498.6 (+0.7)	13970.9 (+0.7)	0.1562 (−1.8)	5876.4 (+1.4)
Running bond	Abaqus	15021.0	14177.0	0.1580	5981.5
	Reuss	13887.2 (−7.5)	13887.2 (−2.0)	0.1671 (+5.8)	5949.5 (−0.5)
	Voigt	15322.1 (+2.0)	15322.1 (+8.1)	0.1548 (−1.9)	6633.8 (+10.9)
	Salamon	15656.7 (+4.2)	14565.3 (+2.7)	0.1589 (+0.6)	6181.9 (+3.4)
	Brooks	–	14157.0 (−0.1)	–	–
	Pande et al.	14988.1 (−0.2)	14282.6 (+0.7)	0.1565 (−0.9)	5949.5 (−0.5)
	Zucchini & Lourenço	–	–	–	5999.2 (+0.3)
	MoC	14966.8 (−0.4)	14178.5 (−)	0.1564 (−0.9)	6350.6* (+6.2)
	MSE	15099.5 (+0.5)	14219.9 (+0.3)	0.1571 (−0.5)	6046.5 (+1.1)

* Improved MSE.

Table 3
Parameters defining the creep functions of bricks and mortar (Eq. (46)) employed in the numerical simulations.

	Brick	Mortar
E [MPa]	17100	7700
G [MPa]	7435	3208
$n=1$		
j_1	0.5327	0.7602
τ_1 [days]	72.33	29.61
$n=2$		
j_1	0.20842	0.60601
τ_1 [days]	1.5051	0.94854
j_2	0.31521	0.15914
τ_2 [days]	68.277	31.259

A priori, the elastic moduli given by the Method of Cells are neither an upper nor a lower bound for the real moduli. Alternatively, the values of the d.o.f.s U_1, U_2, W_1 and W_3 can be obtained by minimizing the total potential energy Π of the RVE (see Eq. (4)). The advantage of this approach is that the strain energy stored in the RVE is underestimated, and the predicted elastic moduli are upper bounds for the real homogenized moduli. Let Π be written in the form

$$\Pi=\frac{1}{2\Delta}\begin{pmatrix}U_1\\U_2\\W_1\\W_3\end{pmatrix}^T\begin{pmatrix}k_{11}&&&\\-k_{22}+\Delta_{12}&k_{22}&\text{symm.}&\\3\alpha_{14}k_{44}-\Delta_{13}&-\alpha_{14}k_{44}&k_{44}+\Delta_{33}&\\-\alpha_{14}k_{44}&-\alpha_{14}k_{44}&-k_{44}&k_{44}\end{pmatrix}\begin{pmatrix}U_1\\U_2\\W_1\\W_3\end{pmatrix}-\Sigma_{11}\frac{U_1+U_2}{b_b+b_m}+\Sigma_{33}\frac{W_1+W_3}{h_b+h_m},\tag{29}$$

where

$$\begin{aligned}k_{11}&=96E'_b\alpha_b^2\alpha_m^2+E'_m(8\alpha_b\alpha_m^2(3+2\alpha_h(1+2\alpha_b(2-\alpha_b)))\\&\quad+\alpha_h(3+11\alpha_b+4(2-\alpha_b)\alpha_b^2)(1-\nu_m)),\\k_{22}&=E'_m(8\alpha_b\alpha_m^2(3+2\alpha_h)+\alpha_h(3-\alpha_b)(1-\nu_m)),\\k_{44}&=24E'_m\alpha_h(1+\alpha_b),\end{aligned}\tag{30}$$

$$\Delta_{12}=2E'_m\alpha_b\alpha_h(8\alpha_b\alpha_m^2-(3-\alpha_b)(1-\nu_m)),\quad \Delta_{13}=96E'_b\alpha_b\alpha_h\alpha_m\nu_b,$$

$$\Delta_{33}=96\alpha_h^2(E'_b+\alpha_bE'_m),\quad \alpha_{14}=\frac{\alpha_b\alpha_m\nu_m}{1+\alpha_b},\quad \Delta=24h_m^2(1+\alpha_b)(1+\alpha_h)$$

and

$$E'_m=\frac{E_m}{1-\nu_m^2},\quad E'_b=\frac{E_b}{1-\nu_b^2}.\tag{31}$$

Minimizing Π with respect to the d.o.f.s and replacing the computed values in Eq. (23), new estimates for the macroscopic elastic constants can be obtained (labeled with MSE hereafter) and read:

$$\begin{aligned}E_1^{(MSE)}&=\frac{1+\alpha_b}{24(\alpha_b\alpha_m)^2(1+\alpha_h)}\frac{a}{b-c},\\E_2^{(MSE)}&=\frac{1+\alpha_h}{24\alpha_h^2(1+\alpha_b)}\frac{ak_{44}}{d(4k_{44}+\Delta_{33})-ck_{22}},\\\nu_{12}^{(MSE)}&=\frac{1+\alpha_b}{\alpha_B(1+\alpha_h)}\frac{e}{b-c},\end{aligned}\tag{32}$$

with

$$\begin{aligned}a&=(k_{11}-k_{22})(k_{22}\Delta_{33}-k_{44}\alpha_{14}^2(4k_{44}+\Delta_{33}))+\left(k_{44}\alpha_{14}^2-\Delta_{12}/2\right)\\&\quad(c+2\Delta_{33}\Delta_{12})+\Delta_{12}\Delta_{13}^2/2-k_{22}\left(2\Delta_{33}(2k_{44}\alpha_{14}^2-\Delta_{12})+\Delta_{13}^2\right),\\b&=(k_{11}+3k_{22}-2\Delta_{12})\Delta_{33},\quad c=(4k_{44}\alpha_{14}-\Delta_{13})^2,\\d&=k_{11}k_{22}-(k_{22}-\Delta_{12})^2,\\e&=4(k_{11}-k_{22}+2\alpha_{14}\Delta_{13}-4k_{44}\alpha_{14}^2)k_{44}\alpha_{14}\\&\quad+(4k_{22}-2\Delta_{12}-\alpha_{14}\Delta_{13})\Delta_{13}+\alpha_{14}b.\end{aligned}\tag{33}$$

Eqs. (26), (27) or (32) can be employed to approximately predict the time evolution of the macroscopic strains under sustained macroscopic stresses. Using the concept of age-adjusted moduli (Bažant, 1972), it is sufficient to assume that E_m and E_b (or their ratio α_E) are time-dependent functions, corresponding to the inverse of the creep function of each phase. In Section 5 it will be assessed to what extent this approximations affects the prediction of the macroscopic creep behavior of masonry under normal stresses.

4.2. Instantaneous and delayed behavior under in-plane shear

A similar approach can be proposed under in-plane shear. According to the finite element solution shown in Fig. 1(c), a strain-periodic displacement field can be formulated over the different sub-cells, which is completely defined by three d.o.f.s U_1, U_2 and W_2 (refer to Fig. 4 for the meaning of the symbols):

$$
\begin{aligned}
&u_1^{(1)} = 2U_1\frac{x_2}{h_b}, \quad u_2^{(1)} = 0; \quad u_1^{(2)} = u_1^{(1)}, \quad u_2^{(2)} = W_1\frac{x_1 - \frac{b_b}{2}}{b_m};\\
&u_1^{(3)} = U_1 + \frac{U_2 - U_1}{h_m}\left(x_3 - \frac{h_b}{2}\right), \quad u_2^{(3)} = -W_2\frac{x_2 - h_b/2}{h_m};\\
&u_1^{(4)} = u_1^{(3)}, \quad u_2^{(4)} = -u_2^{(3)};\\
&u_1^{(5)} = u_1^{(3)}, \quad u_2^{(5)} = -W_1\frac{\left(x_1 - \frac{b_b+b_m}{2}\right)\left(x_2 - \frac{h_b}{2}\right) - h_m\left(x_1 - \frac{b_b}{2}\right)}{b_m h_m};\\
&u_1^{(6)} = u_1^{(3)}, \quad u_2^{(6)} = W_1\frac{x_1(x_2 - h_b/2)}{b_m h_m}
\end{aligned}
\tag{34}
$$

with $W_1 = 2W_2$. Stresses and strains are uniform over the sub-cells, except for the cross joints (sub-cells 5 and 6), similarly to the solution proposed under normal macroscopic stresses. Within these sub-cells, the equilibrium equation along x_1 for an infinitesimal element is not fulfilled.

The macroscopic shear strain associated with the microscopic displacement field (34) is

$$2E_{12} = \frac{2}{|V|}\int_V \epsilon_{12}dV = \frac{U_1 + U_2}{h_b + h_m} + \frac{W_1}{b_b + b_m}. \tag{35}$$

A relationship between U_1 and W_2 can be found by prescribing that equilibrium at the interface between bricks and head joints is fulfilled:

$$\sigma_{12}^{(1)} = \sigma_{12}^{(2)} \;\Rightarrow\; W_2 = U_1\frac{b_m}{h_b}\left(\frac{1}{\alpha_G} - 1\right). \tag{36}$$

Similarly, fulfillment of equilibrium at the interface between sub-cells 1 and 3 (or 1 and 4) yields a relationship between U_1 and U_2:

$$\sigma_{12}^{(1)} = \sigma_{12}^{(3)} \;\Rightarrow\; U_2 = U_1\left(1 + 2\frac{\alpha_h}{\alpha_G}\right). \tag{37}$$

In this way, equilibrium between adjacent sub-cells is not fulfilled only parallel to the boundary of the cross joints, and normally to the interface between brick and bed joint.

The remaining d.o.f., U_1, can be related to the macroscopic shear strain through Eq. (35):

$$2E_{12} = \frac{2}{1 + \alpha_b}\left(1 - \alpha_b\alpha_h + \frac{\alpha_b + \alpha_h + 2\alpha_b\alpha_h}{\alpha_G}\right)\frac{U_1}{h_b + h_m}. \tag{38}$$

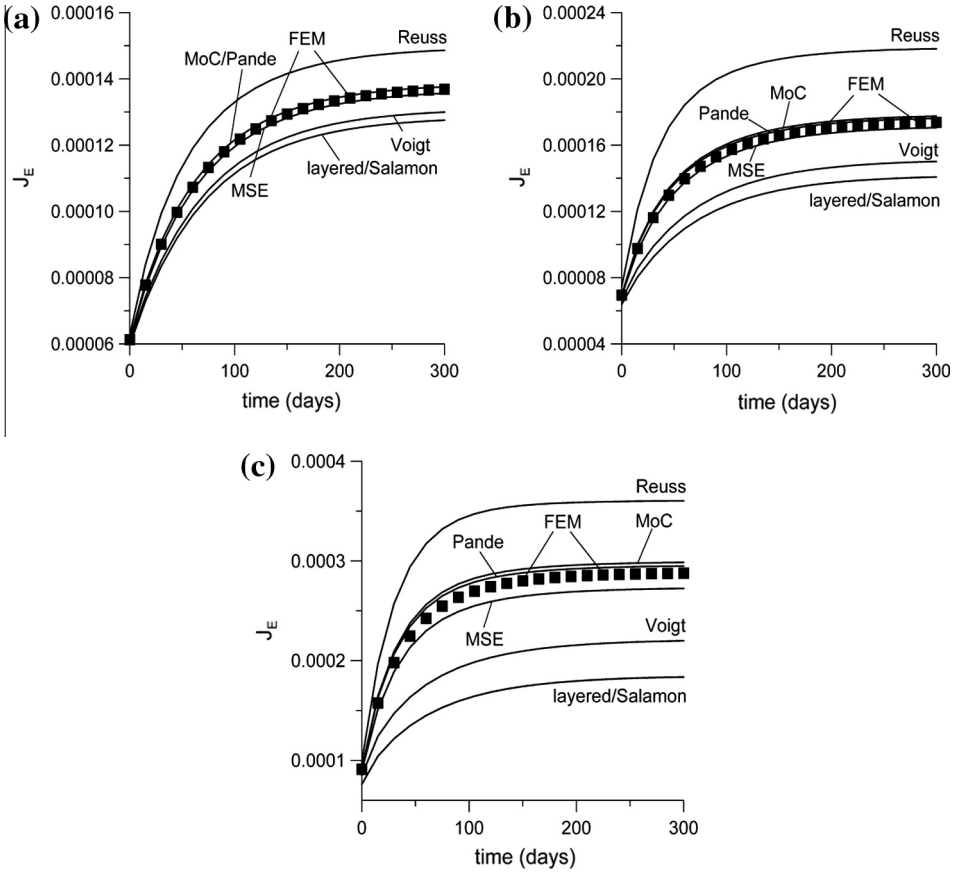

Fig. 7. Creep curves under sustained macroscopic horizontal stress Σ_{11}: comparison between numerical and analytical predictions using Prony series of one term: (a) thin joints, (b) standard joints, and (c) thick joints.

Finally, computing the macroscopic shear stress $\Sigma_{12} = \frac{1}{|V|}\int_V \sigma_{12} dV$, a MoC-type approximated value for the macroscopic in-plane shear modulus G_{12} can be obtained:

$$G_{12}^{(MoC)} = \frac{\Sigma_{12}}{2E_{12}} = G_m\left(1 + \frac{1-\alpha_G}{\alpha_b + \alpha_h + 2\alpha_b\alpha_h + \alpha_G(1-\alpha_b\alpha_h)}\right). \tag{39}$$

This value is found to be smaller than Reuss lower bound to the in-plane shear modulus, Eq. (7). Thus, the approximation provided by the approach followed hitherto, based on the original version of the Method of Cells, is less severe than that given by a simple uniform statically admissible solution. Indeed, the transverse shear modulus obtained by Aboudi (1991) for polymers reinforced by a square doubly periodic array of long fibers coincides with Reuss lower bound.

To improve the approximation, here it is proposed to determine U_1 minimizing the macroscopic strain energy over the RVE, according to Eq. (4):

$$\min_{U_1}\Pi \;\Rightarrow\; U_1 = \frac{3h_m\alpha_G(\alpha_b + \alpha_h + \alpha_b\alpha_h(2-\alpha_G) + \alpha_G)(1-\nu_m)\Sigma_{12}}{G_m\alpha_h\left(\frac{(3-\alpha_b)(1-\alpha_G)^2\alpha_h}{\alpha_m^2} + 2(3(\alpha_G+\alpha_h) + \alpha_b(3 + (11 - 2(5-\alpha_G)\alpha_G)\alpha_h))(1-\nu_m)\right)}. \tag{40}$$

Computing the macroscopic shear strain $E_{12} = \frac{1}{|V|}\int_V \epsilon_{12} dV$, an improved MoC-type approximated value for the in-plane shear modulus of the homogenized material is given by:

$$G_{12}^{(iMoC)} = G_m\frac{(1+\alpha_b)(1+\alpha_h)}{c_3c_4}(c_4 + (1-\alpha_G)\alpha_h((3-\alpha_b)(1-\alpha_G) - 2\alpha_b\alpha_m^2(1-\nu_m)(2\alpha_G - 5))), \tag{41}$$

where

$$c_3 = \alpha_b + \alpha_h + \alpha_G + \alpha_b\alpha_h(2-\alpha_G), \quad c_4 = 6c_3\alpha_m^2(1-\nu_m). \tag{42}$$

Eq. (41) gives an upper bound for the macroscopic shear modulus of masonry.

Alternatively, the values of all the parameters U_1, U_2 and W_2 that define the displacement field over the RVE can be obtained by minimizing the macroscopic potential energy over the RVE:

$$\begin{aligned} U_1 &= \frac{h_m(1+\alpha_b)(c_1+c_2)\alpha_G}{2G_m\alpha_h((1+\alpha_b\alpha_G)c_1 + (1+\alpha_b)c_2)}\Sigma_{12}, \\ U_2 &= \frac{h_m(2\alpha_h(1+\alpha_b\alpha_G) + \alpha_G(1+\alpha_b))(c_1+c_2)}{2G_m\alpha_h((1+\alpha_b\alpha_G)c_1 + (1+\alpha_b)c_2)}\Sigma_{12}, \\ W_2 &= \frac{3h_m(1+\alpha_b)(1-\alpha_G)\alpha_b\alpha_m(1-\nu_m)}{G_m((1+\alpha_b\alpha_G)c_1 + (1+\alpha_b)c_2)}\Sigma_{12}, \end{aligned} \tag{43}$$

with

$$\begin{aligned} c_1 &= \alpha_h(3 + \alpha_b(2-\alpha_b)(1 + 2\alpha_m^2(1-\nu_m))), \\ c_2 &= 6\alpha_b\alpha_m^2(1-\nu_m). \end{aligned} \tag{44}$$

Again, computing the macroscopic shear strain as average of the microscopic strains, a stricter upper bound to the real macroscopic shear modulus can be obtained:

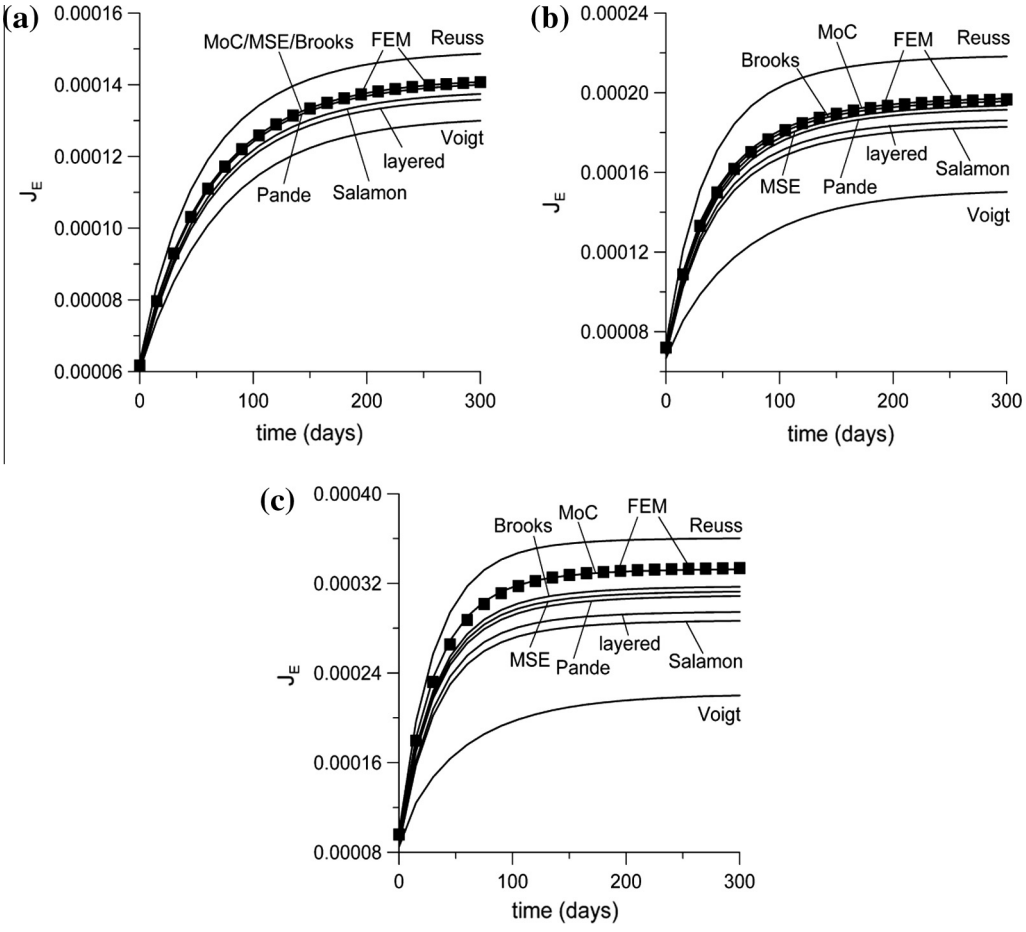

Fig. 8. Creep curves under sustained macroscopic vertical stress Σ_{22}: comparison between numerical and analytical predictions using Prony series of one term: (a) thin joints, (b) standard joints, and (c) thick joints.

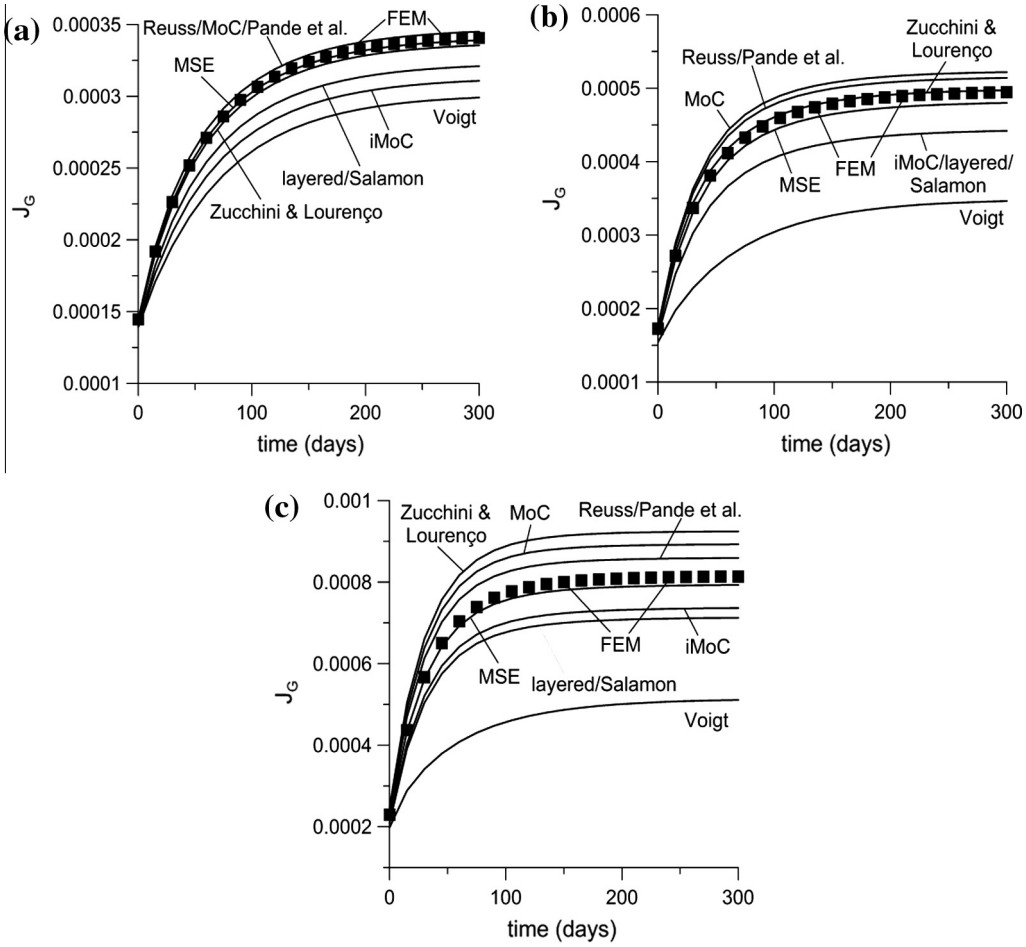

Fig. 9. Creep curves under sustained macroscopic simple shear Σ_{12}: comparison between numerical and analytical predictions using Prony series of one term: (a) thin joints, (b) standard joints, and (c) thick joints.

$$G_{12}^{(MSE)} = G_m \left(1 + \frac{1-\alpha_G}{\alpha_h + \alpha_b(1+\alpha_h)\left(1 - \frac{(1-\alpha_G)c_1}{c_1+c_2}\right) + \alpha_G} \right). \tag{45}$$

A disadvantage of the latter approach is that equilibrium at the interfaces is not fulfilled *a priori*, contrary to the approach that led to Eq. (41). Although Eq. (41) is less accurate than Eq. (45), the stress field on which Eq. (41) is based could be employed in future extensions of this research, e.g., to derive macroscopic strength criteria according to a static limit analysis approach.

Again, using the concept of age-adjusted (or effective) shear moduli, Eqs. (39), (41), and (45) can be extended to predict the time evolution of the macroscopic shear strains under sustained shear stress by simply replacing the constant ratio α_G by a time-dependent ratio $\alpha_G(t) = J_b(t)(1+\nu_b)/(J_m(t)(1+\nu_m))$. The reliability of this approximation will be assessed in Section 5.

5. Numerical applications

Several parametric investigations were carried out to assess the accuracy of the closed-form expressions for the macroscopic elastic an creep coefficients derived in Section 4 through comparisons with refined FE solutions. All the numerical analyses (both elastic and viscoelastic) were carried out using the commercial FE code Abaqus. The macroscopic coefficients derived hitherto are also compared with the Voigt and Reuss bounds (Section 2.2) and with other expressions available in the literature (see Section 3 and Appendix A).

5.1. Macroscopic elastic properties

The values of the geometrical and elastic parameters employed in the applications shown in this Section are summarized in Table 1. In the first column, the number of the figure in which the different sets of parameters were used is reported. The geometric parameters correspond to header bond brickwork. In all the applications, the elastic parameters of mortar are $E_m = 7700$ MPa, $\nu_m = 0.2$ (and $G_m = 3208.3$ MPa). The Poisson's ratio of the brick is $\nu_b = 0.15$.

In Fig. 5 the influence of the material heterogeneity (quantified by the ratio of the mortar Young's modulus or shear modulus to the corresponding brick modulus, α_E or α_G) on the predicted values of the macroscopic in-plane elastic moduli, Poisson's ratio and shear modulus is investigated for header bond brickwork with standard (10 mm thick) joints. Under normal stress (Fig. 5(a)–(c)), both the original MoC (Eqs. (26) and (27)) and Pande's theory (Eq. (47)) match the FE results with the same degree of accuracy; the expressions obtained minimizing the potential energy of the RVE, Eq. (32), fit the numerical results with higher accuracy. It must be acknowledged, however, that the vertical elastic modulus is predicted fairly well by most of the expressions available in the literature (Fig. 5(b)), including a simple layered model. Eq. (32) gives also the best agreement in terms of numerically computed Poisson's ratio (Fig. 5(c)). Under in-plane shear, the most accurate predictions are given by the minimization of potential energy (Eq. (45)); Zucchini and Lourenço's formula, Eq. (20), gives the best agreement with the numerical results if the shear moduli of brick and mortar are not too different ($\alpha_G > 0.4$).

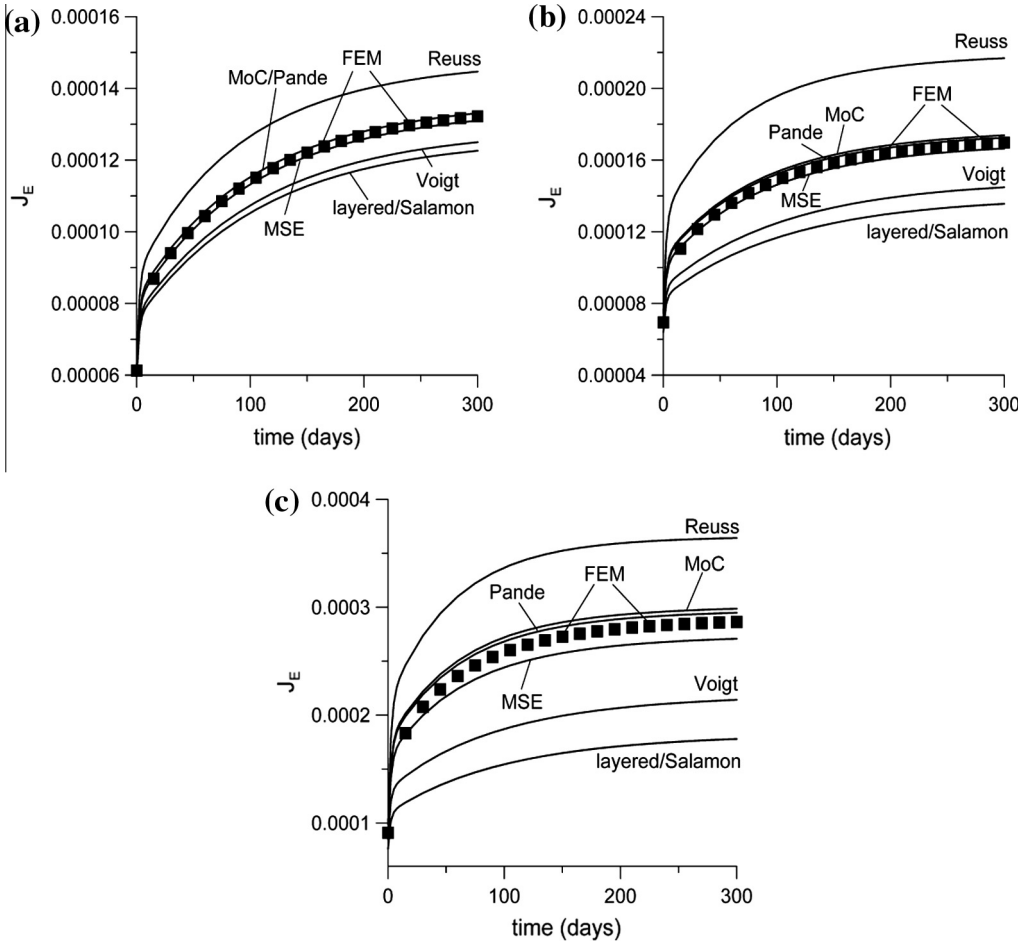

Fig. 10. Creep curves under sustained macroscopic horizontal stress Σ_{11}: comparison between numerical and analytical predictions using Prony series of two terms: (a) thin joints, (b) standard joints, and (c) thick joints.

In Fig. 6 the influence of the joint thickness-to-brick height ratio on the macroscopic in-plane elastic parameters of header bond brickwork is investigated. As this ratio increases, the original MoC gives the better predictions in terms of vertical elastic modulus (Fig. 6(b)), whereas the minimization of the potential energy better fits the numerically computed horizontal elastic modulus and shear modulus (Fig. 6(a) and (d)). Additionally, note that for thick joints the predictions by Zucchini and Lourenço are less accurate than those derived here or those proposed by Pande et al. For thick joints, the numerically computed Poisson's ratio is not correctly predicted by any of the available expressions (Fig. 6(c)).

Finally, in Table 2 the influence of the brick aspect ratio $\alpha_B = h_b/b_b$ on the approximated macroscopic moduli is investigated. Header bond brickwork ($\alpha_B = 55/120 = 0.4583$) and running bond brickwork ($\alpha_B = 55/250 = 0.22$) with standard (10 mm thick) joints were considered. The predictions obtained with the layered model are not reported, as they are very close to, or even coincide with, Salamon's predictions. Minimization of the potential energy with respect to all the d.o.f.s gives very good estimates for the numerically computed macroscopic moduli. Note, however, that for the selected values of the geometric and elastic parameters, the FE results are well matched also by most of the existing proposals.

5.2. Macroscopic creep behavior

The possibility of predicting the delayed macroscopic strains of a masonry element under sustained macroscopic stresses is now assessed by simply replacing the inverse of the elastic moduli of units and mortar by the creep functions of the two components, $J_b(t)$ and $J_m(t)$, according to the concept of effective age-adjusted modulus (Bažant, 1972). The so-called generalized Maxwell's rheological model, which basically consists of n Maxwell elements in parallel with an elastic spring (see e.g., Kaliske and Rothert, 1997), is employed to describe the time evolution of creep strains in units and mortar. Accordingly, both $J_b(t)$ and $J_m(t)$ can be cast in the form:

$$J(t) = \frac{1}{E_\infty}\left(1 - \sum_{i=1}^{n} j_i \exp(-t/\tau_i)\right), \tag{46}$$

where E_∞ is the delayed modulus of the material, which is related to the instantaneous (elastic) modulus E by $E_\infty = E(1 - \sum j_i)$, j_i are non-dimensional creep moduli and τ_i are called creep times. The r.h.s. in Eq. (46) is usually referred to as a Prony series expansion. In the applications shown hereafter, the coefficients j_i and τ_i were given values obtained by best fitting the data of creep tests on mortar samples and calcium silicate bricks carried out by Brooks (1990)): these values are listed in Table 3 (see also Taliercio, 2013). The Poisson's ratios ν_b and ν_m are supposed to be constant in time: readers are referred e.g., to Loo and Base (1990) for a discussion on the reliability of this assumption. Again, the accuracy of the theoretical predictions is assessed assuming the macroscopic creep curves obtained using a refined FE model of any RVE as a benchmark. The FE code Abaqus employed in the numerical

analyses integrates the constitutive law over time, explicitly taking the stress redistribution over the two components into account.

Figs. 7–9 show the macroscopic creep coefficients for header bond brickwork with thin (2 mm), standard (10 mm) and thick (40 mm) mortar joints, under sustained horizontal stress (Figs. 7(a), 8(a) and 9(a)), vertical stress (Figs. 7(b), 8(b) and 9(b)), and in-plane shear (Figs. 7(c), 8(c) and 9(c)). These coefficients were computed both according to the expressions derived in Section 4 and adapting expressions for the macroscopic elastic properties of masonry available in the literature to the prediction of the macroscopic creep coefficients using age-adjusted moduli. Figs. 7–9 refer to the case $n = 1$: the corresponding rheological model is also called Zener model. Remarks similar to those made in Section 5.1 apply. For thin joints, all the expressions taking head joints into account (MoC, MSE, Pande et al., Brooks, Zucchini & Lourenço) basically fit the numerical predictions with the same accuracy. The macroscopic vertical creep estimated according to the original MoC are quite accurate, both for standard and for thick mortar joints. The macroscopic horizontal and shear creep strains are better matched by the estimates based on the minimization of the potential energy. The macroscopic shear creep strains computed according to Zucchini & Lourenço's model are accurate for standard joint, but not for thick joints.

To assess whether the same conclusions can be drawn using more complex creep functions, the same numerical simulations referred to in Figs. 7–9 were carried out using Prony series of two terms. Incidentally, note that with $n = 2$ experimental creep tests on calcium silicate bricks and mortar samples can be reproduced with fair accuracy (Taliercio, 2013). The results obtained are shown in Figs. 10–12. Again, the minimization of the potential energy gives the best agreement with the numerical results under horizontal stress or shear, whereas the original MoC is more accurate as far as the evolution of the creep strains under vertical stress is concerned. If joints are thin, the various expressions derived taking head joints into account are equally accurate.

6. Concluding remarks

Using a kinematic approach inspired by the Method of Cells (MoC) for fiber reinforced composites, having affinities with the approach proposed by Zucchini and Lourenço (2002), closed form expressions for all the macroscopic in-plane elastic constants of regular pattern masonry were derived, with different degrees of accuracy (Section 4). Note that most models available in the literature (Section 3) give analytical expressions only for some of the constants. According to the numerical applications (Section 5.1), the expressions obtained for the macroscopic elastic moduli using the original Method of Cells, Eqs. (26) and (27), or the minimization of the potential energy of any RVE, Eq. (32), are basically found to be equally accurate for header bond brickwork, for any joint thickness and stiffness of the units. As the expressions for the moduli computed according to the original MoC are much simpler, for practical purposes it is advisable to use Eqs. (26) and (27) rather than Eq. (32). The minimization of the potential energy gives

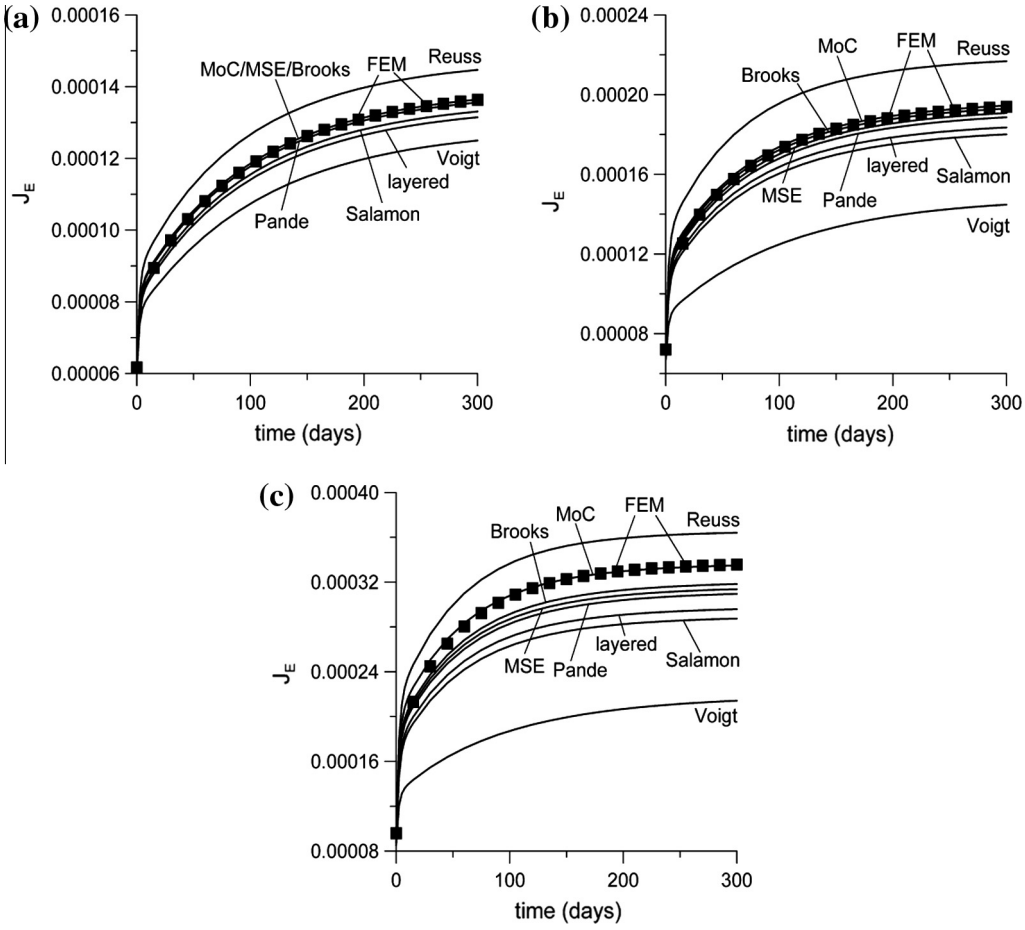

Fig. 11. Creep curves under sustained macroscopic vertical stress Σ_{22}: comparison between numerical and analytical predictions using Prony series of two terms: (a) thin joints, (b) standard joints, and (c) thick joints.

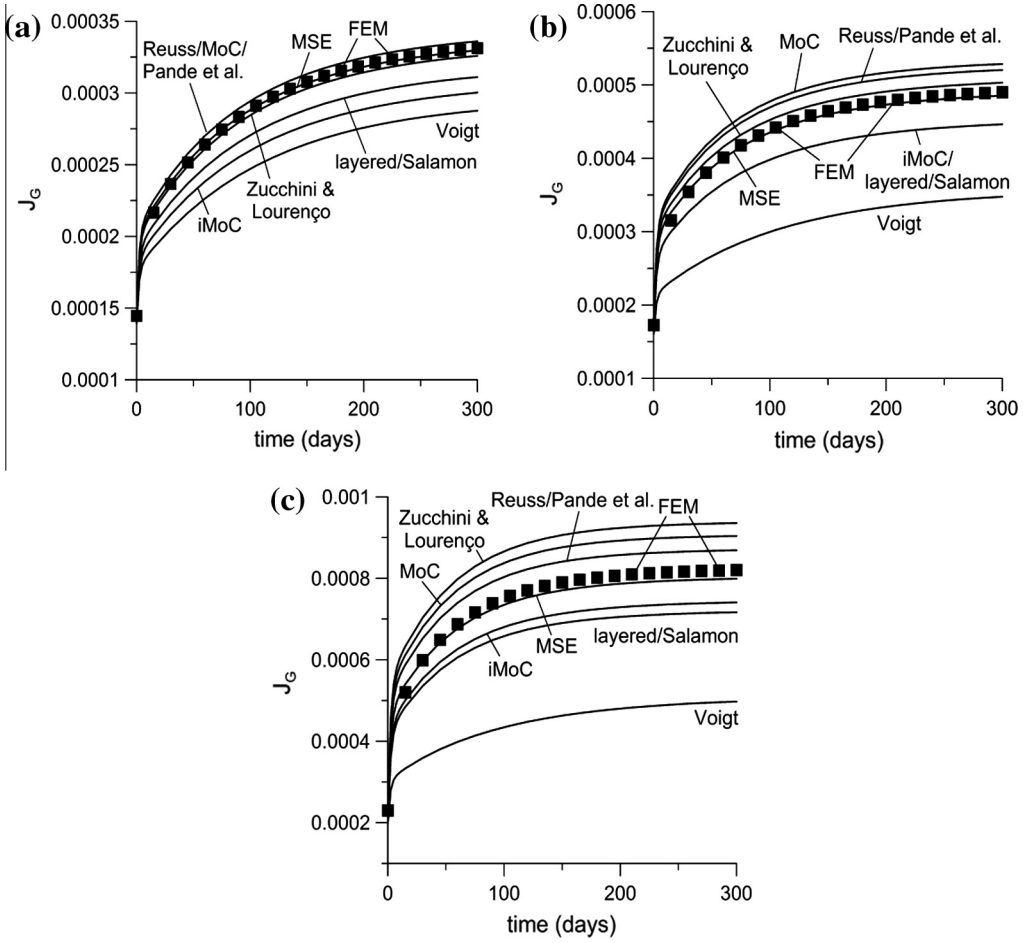

Fig. 12. Creep curves under sustained macroscopic simple shear Σ_{12}: comparison between numerical and analytical predictions using Prony series of two terms: (a) thin joints, (b) standard joints, and (c) thick joints.

somewhat more accurate results in terms of horizontal Young's modulus. Conversely, minimizing the potential energy of any RVE the most accurate predictions for the elastic shear modulus are obtained (Eq. (45)).

The proposed expressions for the macroscopic elastic constants can also be used to derive the in-plane macroscopic creep coefficients of masonry, using the concept of effective modulus: these coefficients were numerically shown to match the finite element simulation of creep tests on a RVE accurately, both under normal stresses and shear (Section 5.2), for any joint thickness. Again, the expressions obtained using the MoC in its original form are appropriate as far as the vertical creep behavior is concerned. Under sustained shear stress, the expression of the creep coefficient based on the minimization of the potential energy are more accurate.

Comparisons with theoretical expressions available in literature have shown that in most instances the expressions derived in the present work are globally more accurate over the entire range of material elastic moduli and joint thicknesses explored in the numerical applications.

In the continuation of this research, the proposed approach will be extended to different types of brick patterns (English bond, Flemish bond, etc.), which require a different choice for the geometry of the RVE. Unlike the case considered here (header or running bond brickwork), according to previous studies (Anthoine, 1997; Taliercio, 2013) the state of stress within the RVE cannot be assumed to be plane if stretchers and headers coexist in the wall. The microscopic displacement field employed in Section 4.1 could also be improved to obtain better predictions for the macroscopic Poisson's ratio if joints are thick. Finally, the approach proposed hitherto could be extended to the prediction of the out-of-plane stiffness of brick walls, which is of particular importance under horizontal (e.g., seismic) loads. Macroscopic strength criteria for in-plane loaded walls could also be formulated using a micromechanical approach based on the expressions of the microscopic stress fields employed in this work to derive the macroscopic elastic and creep coefficients.

Appendix A. Equivalent elastic properties for brick masonry in plane stress according to Pande et al. (1989)

Let the macroscopic 2D constitutive law for the orthotropic medium equivalent to linear elastic brickwork be written as in Eq. (3). According to Pande et al. (1989), the macroscopic elastic constants are given by:

$$E_1^{Pande} = \sum_{i=1}^{2} p_i E'_{1i}, \quad E_2^{Pande} = \left(\sum_{i=1}^{2} \frac{p_i}{E'_{1i}} \left(\frac{E'_{1i}}{E'_{2i}} - 2\nu_i'^2 \right) + \frac{2(\nu_{12}^{Pande})^2}{E_1^{Pande}} \right)^{-1}$$

$$\nu_{12}^{Pande} = \sum_{i=1}^{2} p_i \nu'_i, \quad G_{12}^{Pande} = \left(\sum_{i=1}^{2} \frac{p_i}{G'_k} \right)^{-1} \tag{47}$$

with

$$p_1 = \frac{\alpha_h}{1+\alpha_h}, \quad p_2 = \frac{1}{1+\alpha_h}, \quad E'_{11} = E'_{21} = E_m,$$

$$E'_{12} = E_m \quad p_m(1-2\nu_m^2) + p_b\alpha_E(1-2\nu_b^2) + 2\frac{(p_m\nu_m + p_b\nu_b)^2}{p_m + p_b/\alpha_E}\Bigg)^{-1},$$

$$E'_{22} = E_m(p_m + p_b/\alpha_E),$$

$$\nu'_1 = \nu_m, \quad \nu'_2 = (p_m\nu_m + p_b\nu_b)\frac{E'_{12}}{E'_{22}}, \quad G'_1 = G_m,$$

$$G'_2 = G_m(p_m + p_b\alpha_G)^{-1} \tag{48}$$

having set $p_m = \alpha_b/(1+\alpha_b)$ and $p_b = 1/(1+\alpha_b)$.

Appendix B. Symbology

- h_b = brick height,
- b_b = brick width,
- h_b = bed joint thickness,
- b_m = head joint thickness,
- E_b = brick Young's modulus,
- E_m = mortar Young's modulus,
- ν_b = brick Poisson's ratio,
- ν_m = mortar Poisson's ratio,
- $G_b = E_b/(2(1+\nu_b))$ = brick shear modulus,
- $G_m = E_m/(2(1+\nu_m))$ = mortar shear modulus,
- $\alpha_h = h_m/h_b$,
- $\alpha_b = b_m/b_b$,
- $\alpha_B = h_b/b_b$ = brick aspect ratio ($=\alpha_m\alpha_b/\alpha_h$),
- $\alpha_m = h_m/b_m$,
- $\alpha_E = E_m/E_b$,
- $\alpha_G = G_m/G_b$,
- $\eta_b = \frac{1}{1+\alpha_b+\alpha_h+\alpha_b\alpha_h}$ = brick volume fraction,
- $\eta_m = \frac{\alpha_b+\alpha_h+\alpha_b\alpha_h}{1+\alpha_b+\alpha_h+\alpha_b\alpha_h} = 1-\eta_b$ = mortar volume fraction.

References

Aboudi, J., 1991. Mechanics of composite materials – A unified micromechanical approach. In: Studies in Applied Mechanics. vol. 29. Elsevier, Amsterdam.

Anthoine, A., 1995. Derivation of the in-plane elastic characteristics of masonry through homogenization theory. Int. J. Solids Struct. 32 (2), 137–163.

Anthoine, A., 1997. Homogenization of periodic masonry: plane stress, generalized plane strain or 3D modeling? Commun. Numer. Methods Eng. 13, 319–326.

Bažant, Z.P., 1972. Prediction of concrete creep effects using age-adjusted effective modulus method. Proc. Am. Concr. Inst. 69, 212–217.

Brooks, J.J., 1986. Composite models for predicting elastic and long-term movements in brickwork walls. Proc. Br. Masonry Soc. 1, 20–23.

Brooks, J.J., 1990. Composite modeling of masonry deformation. Mater. Struct. 23, 241–251.

Cecchi, A., Tralli, A., 2012. A homogenized viscoelastic model for masonry structures. Int. J. Solids Struct. 49 (13), 1485–1496.

Cluni, F., Gusella, V., 2004. Homogenization of non-periodic masonry structures. Int. J. Solids Struct. 41 (7), 1911–1923.

Hughes, T.G., Harvey, R.J., 1995. Creep measured in a brick masonry tower block. Masonry Int. 9 (2), 50–56.

Kaliske, M., Rothert, H., 1997. Formulation and implementation of three-dimensional viscoelasticity at small and finite strains. Comput. Mech. 19 (3), 228–239.

Loo, Y.H., Base, G.D., 1990. Variation of creep Poisson's ratio with stress in concrete under short-term uniaxial compression. Mag. Concr. Res. 42 (151), 67–73.

Luciano, R., Sacco, E., 1998. Damage of masonry panels reinforced by FRP sheets. Int. J. Solids Struct. 35 (15), 1723–1741.

Milani, G., Lourenço, P.B., Tralli, A., 2006. Homogenised limit analysis of masonry walls. Part I: failure surfaces. Comput. Struct. 84 (3–4), 166–180.

Nemat-Nasser, S., Hori, M., 1993. Micromechanics: Overall Properties of Heterogeneous Materials. North-Holland, London.

Pande, G.N., Liang, J.X., Middleton, J., 1989. Equivalent elastic moduli for brick masonry. Comput. Geotech. 8, 243–265.

Park, S.W., Schapery, S.A., 1999. Methods of interconversion between linear viscoelastic material functions. Part I – A numerical method based on Prony series. Int. J. Solids Struct. 36 (11), 1653–1675.

Pietruszczak, S., Niu, X., 1992. A mathematical description of macroscopic behavior of brick masonry. Int. J. Solids Struct. 29 (5), 531–546.

Reda Taha, M.M., Shrive, N.G., 2006. A model of damage and creep interaction in a quasi-brittle composite material under axial loading. J. Mech. 22 (4), 339–347.

Sacco, E., 2009. A nonlinear homogenization procedure for periodic masonry. Eur. J. Mech. A Solids 28 (2), 209–222.

Salamon, M.D.G., 1968. Elastic moduli of a stratified rock mass. Int. J. Rock Mech. Min. Sci. 5, 519–527.

Sayed-Ahmed, E.Y., Shrive, N.G., Tilleman, D., 1998. Creep deformation of clay masonry structures: a parametric study. Can. J. Civ. Eng. 25 (1), 67–80.

Shieh-Beygi, B., Pietruszczak, S., 2008. Numerical analysis of structural masonry: mesoscale approach. Comput. Struct. 86 (21–22), 1958–1973.

Shrive, N.G., Sayed-Ahmed, E.Y., Tilleman, D., 1997. Creep analysis of clay masonry assemblages. Can. J. Civ. Eng. 24, 367–379.

Taliercio, A., 2013. Analysis of the behavior of brick masonry with calcium silicate units under sustained loads. Masonry Int. 26 (1), 17–26.

Zhao, Y.H., Weng, G.J., 1990. Effective elastic moduli of ribbon-reinforced composites. ASME J. Appl. Mech. 57, 158–167.

Zucchini, A., Lourenço, P.B., 2002. A micro-mechanical model for the homogenization of masonry. Int. J. Solids Struct. 39 (12), 3233–3255.

Zucchini, A., Lourenço, P.B., 2007. Mechanics of masonry in compression: results from a homogenization approach. Comput. Struct. 85, 193–204.